applied sciences

MDPI

Article

Advanced Numerical Analysis of Transport Packaging

Aram Cornaggia [1], Damian Mrówczyński [2], Tomasz Gajewski [3], Anna Knitter-Piątkowska [3] and Tomasz Garbowski [4,*]

[1] Department of Engineering and Applied Sciences, Università degli studi di Bergamo, Viale G. Marconi 5, 24044 Dalmine, BG, Italy; aram.cornaggia@unibg.it
[2] Doctoral School, Poznan University of Life Sciences, Wojska Polskiego 28, 60-637 Poznań, Poland; damian.mrowczynski@up.poznan.pl
[3] Institute of Structural Analysis, Poznan University of Technology, Piotrowo 5, 60-965 Poznań, Poland; tomasz.gajewski@put.poznan.pl (T.G.); anna.knitter-piatkowska@put.poznan.pl (A.K.-P.)
[4] Department of Biosystems Engineering, Poznan University of Life Sciences, Wojska Polskiego 50, 60-627 Poznań, Poland
* Correspondence: tomasz.garbowski@up.poznan.pl

Abstract: This article presents an extended numerical approach for evaluating the dynamic response of corrugated cardboard transport packaging under simulated transport conditions. Building upon a simplified method previously introduced, this study integrates a more comprehensive Finite Element Analysis (FEA) framework to capture the non-linear behaviour of packaging subjected to vertical random vibrations. The proposed model employs dynamic, modal, and contact analyses to simulate the deformation of packaging and subsequent strength reduction over multiple impact cycles, reflecting real-world conditions more accurately. The developed approach gives detailed insights into the structural degradation of packaging due to repetitive transport loads and validates the findings through comparative compression tests. The results show that enhanced numerical methods improve the accuracy of load-bearing predictions, thereby supporting optimisation in packaging design for various geometries and transport scenarios. This method offers a valuable tool for evaluating the sustainability and cost-effectiveness of packaging solutions in logistics.

Keywords: corrugated board; finite element analysis; dynamic load simulation; transport packaging; structural degradation; material modelling

check for updates

Citation: Cornaggia, A.; Mrówczyński, D.; Gajewski, T.; Knitter-Piątkowska, A.; Garbowski, T. Advanced Numerical Analysis of Transport Packaging. *Appl. Sci.* **2024**, *14*, 11932. https://doi.org/10.3390/app142411932

Academic Editor: Arkadiusz Gola

Received: 16 November 2024
Revised: 13 December 2024
Accepted: 18 December 2024
Published: 20 December 2024

1. Introduction

Paper is a multipurpose material that is scarcely given a second thought when it is used, for example, in cleansing, writing, printing, packing, communicating, or even decorating. In general, paper is manufactured from cellulose fibres, annual plants, and recycled materials such as waste paper [1]. Corrugated paperboard is a material consisting of a fluted corrugated sheet and flat linerboards [2]. The designers of corrugated paper have implemented a principle that posits that, to maintain heavy loads, the most effective way is to use an arch, as in construction [3]. Therefore, thanks to its structure, corrugated board presents many advantages, e.g., durability, good performance, and light weight. The most prevalent layouts have two to seven layers.

For the assessment of the load bearing capacity of corrugated cardboard boxes, an analytical approach can be applied. In the literature, one can find equations that have been developed over time, ranging from the most basic [4–6], which are suitable for standard box design, to the most recent and advanced [7–12]. Recognised and widely used techniques can also include hybrid [7,13,14] or simply numerical [15,16] procedures implementing the Finite Element Method (FEM). Various laboratory tests are also used to assess the mechanical properties of corrugated boards. In order to standardise procedures, a number of typical tests have been established. The predominant ones are the Box Compression Test (BCT) [7,17] and Edge Crush Test (ECT) [18,19], as well as Artificial Intelligence (AI) [20],

which can also be successfully used to identify the geometric features of corrugated cardboard [21]. To record the set of data from the outer surface of the examined specimen, contactless methods such as video extensometry [22] or Digital Image Correlation (DIC) [23] can be utilised. The fundamental examination used in the corrugated packaging sector to evaluate the resistance of a certain package against dynamic load is the Vertical Random Vibration (VRV) test [24]. Among the physical tests that can be conducted on cardboard, the Bending stiffness Test (BNT), Shear Stiffness Test (SST), and Torsional Stiffness Test (TST) should also be mentioned.

The layered structure of corrugated cardboard determines the occurrence of two in-plane directions of orthotropy related to the mechanical strength of paperboard. The Machine Direction (MD) is perpendicular to the main axis of the fluting and parallel to the cardboard fibre arrangement, whereas the Cross Direction (CD) is parallel to the fluting. Moreover, paper, which is a component of each ply of the board, is itself an anisotropic material, and this makes determining the material parameters of each layer a challenging task. The method that allows for replacing a multi-layered structure with a single-layered one, with equivalent properties, is called homogenisation. The finite element approach is the foundation for numerical homogenisation, the most widely used technique that has been extensively applied in recent years to corrugated paperboards [16,25–27], as this procedure provides significant savings in computing time whilst retaining the accuracy of the results.

Corrugated cardboard boxes are most often used in the packaging and transport industries. To protect fragile goods during shipping or storage, the boxes must meet certain conditions of load bearing capacity. The strength of cardboard packaging is fundamental, especially since it is usually exposed to dynamic loads during transport. Only a limited number of studies address the dynamic properties of packaging or corrugated boards, e.g., [28,29]; therefore, this research, as an extension of the simplified approach presented by the authors in [30], is particularly innovative and valuable. Mrówczyński et al. [30] developed a simplified method to assess the dynamic strength of corrugated board boxes. This approach involved static compressive strength measurements, frequency domain analysis of random vibrations to find resonance frequencies, and then dynamic analysis. The numerical models were validated by laboratory testing on three-layer cardboard boxes, proving the method efficacy in calculating the load capacity of diverse packages under dynamic transport loads. Building on this basic work, the technique was refined in two key areas: (1) testing hybrid corrugated board compositions with different fluting and liner materials and (2) enhanced numerical modelling. By examining the effects of these materials on dynamic load resistance, more sustainable and cost-effective packaging options were created without sacrificing strength. This strategy is consistent with the increased emphasis on sustainability in the packaging sector [31,32], addressing the demand for decreased material consumption and lower prices while retaining superb performance [33,34].

Augmented numerical modelling is another important area of advancement presented in the paper. Incorporating machine learning methods into the modelling process improved the accuracy of failure site predictions and optimised box geometries in real time. These algorithms were trained utilising large datasets derived from both laboratory tests and simulations, which increased the prediction capacity of the models [15,16,34,35]. This integration enabled the quick customisation of package designs to individual requirements, resulting in maximum performance under dynamic load situations. In addition to these technological improvements, the proposed model employs dynamic, modal, and contact analyses to simulate the packaging deformation and subsequent strength reduction over multiple impact cycles, reflecting real-world conditions more accurately [36–39].

Traditional dynamic analysis with FEM for VRV testing in the time domain is highly computationally expensive. To address this, we proposed the Power Spectral Density (PSD)-based method [40] to solve a substitute dynamic problem in the frequency domain, providing a solution to the original time-domain problem. The approach for evaluating the dynamic strength of corrugated packaging has been greatly improved by the proposed

research directions. The performance and longevity of packaging solutions have been enhanced through the use of sophisticated numerical modelling and material optimisation. While enhanced vibration analysis has allowed for a more thorough understanding of package behaviour under real-world situations, the integration of machine learning algorithms has allowed for real-time optimisation and more precise failure predictions. This paper describes a complete method for improving the dynamic strength analysis of corrugated board packaging, with the ultimate goal of creating more effective, sustainable, and dependable packaging solutions for the transportation industry. This research leads to the evolution of packaging technology by utilising material innovation and advanced modelling approaches, and by placing an emphasis on sustainability, ensuring the safe and efficient transportation of goods while minimising environmental impacts.

The comprehensive methodology results in a more accurate assessment of packing durability and dependability throughout transportation. Furthermore, in the future, Life Cycle Assessment (LCA) will be included into the package design process. LCA estimates the environmental effect of packaging materials and designs across their full life cycle, from manufacturing to disposal [41,42]. LCA, combined with dynamic strength analysis, leads to the creation of packaging options that are both strong and ecologically friendly. This guarantees that packaging not only protects goods adequately, but also reduces environmental impacts, in line with global sustainability objectives. However, by incorporating life cycle analysis, packaging solutions are guaranteed to be eco-friendly and satisfy the packaging industry increasing demand for sustainable practises.

Apart from the Introduction, the paper is organised as follows: Section 2 introduces the materials and methods, with a workflow of the study (Section 2.1), mechanical tests of the cardboards descriptions (Section 2.2), and an estimation of the packaging resistance to transport loads (Section 2.3). The results of the research are presented in Section 3, and discussed in Section 4. Finally, conclusions are drawn in Section 5.

2. Materials and Methods

2.1. Workflow of the Study

This study analysed the impact of the selected corrugated cardboard material on the decrease in the compressive load bearing capacity of packaging after a cycle of standard transportation loads. Thirteen types of corrugated cardboard materials and three packaging designs were considered, as shown in Figure 1. A variety of corrugated cardboards with different material parameters were selected (the first "For" loop for the (i) index in Figure 1). Section 2.2 discusses the material testing of the cardboards in detail, including sample preparation, test procedures, and the results obtained.

The packages chosen were typical flap boxes, commonly known as American boxes, with various dimensions: (I) 250 × 250 × 150 mm, (II) 300 × 200 × 250 mm and (III) 300 × 200 × 450 mm (the second "For" loop for (j) index in Figure 1).

The compressive load bearing capacity of the packaging was determined through computer simulations using Finite Element Analysis (FEA), which was used in previous studies by the research group; see [39]. The adopted modelling approach is detailed in [30]. In the current study, the initial static compressive load bearing capacity, BCT_0^{ij}, as shown in Figure 1, was first calculated (bottom left). Next, dynamic computations were performed for each packaging, taking into account standard transport loads in accordance with ISO 13355 [24]. The examined packaging, showing permanent deformations due to the applied material model with plasticity and dynamic transport loads, was subsequently subjected to static FEA to calculate BCT^{ij}, as shown in Figure 1 (bottom right). The proposed procedure will be presented in more detail in Section 2.3. Finally, Equation (1) was applied to determine ΔBCT^{ij}, interpreted as the percentage decrease in the compressive load bearing capacity of the packaging after the transportation load cycle:

$$\Delta BCT^{ij} = 100 \cdot \frac{\left| BCT_0^{ij} - BCT^{ij} \right|}{BCT_0^{ij}}. \quad (1)$$

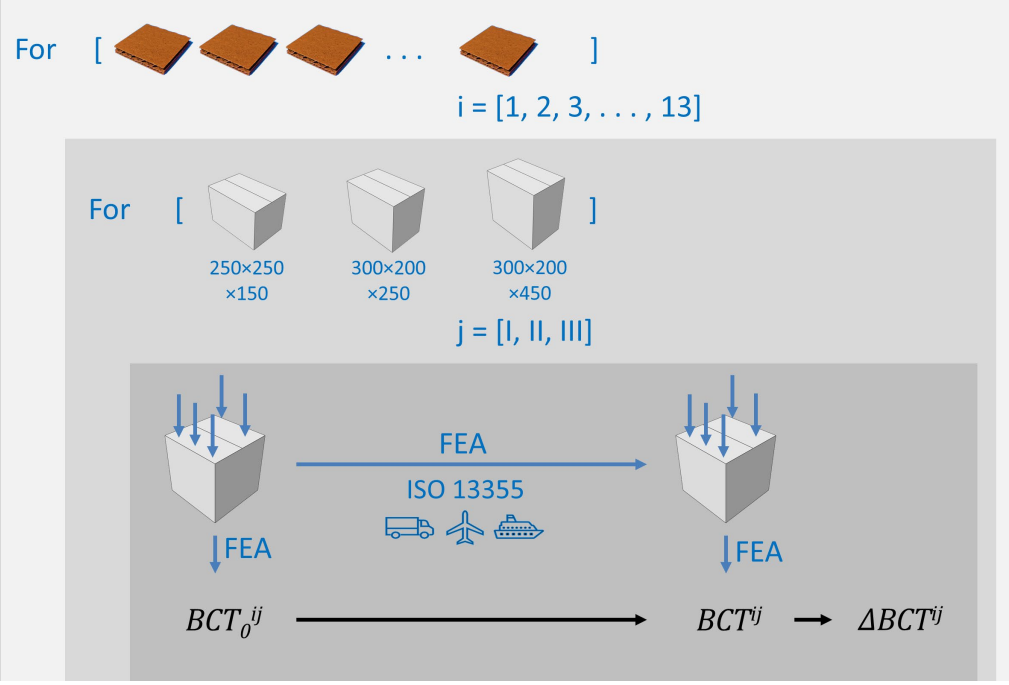

Figure 1. Schematic presentation of the workflow of this study.

2.2. Mechanical Tests on the Cardboards

A crucial aspect of this scientific work is the verification of the influence of corrugated cardboard material on the decrease in compressive strength of packaging subjected to prior transport loads. To achieve this, a series of material tests on corrugated cardboard were conducted, providing material data for computer simulations utilising the finite element method.

In the initial phase, nine types of corrugated cardboard with varied properties were selected, distinguished by differences in the thickness of the constituent papers and the height of the flutes. In the second phase, four additional types of corrugated cardboard were tested to verify the relations observed in the first phase. The cardboard samples were chosen to achieve maximum diversity in mechanical characteristics. The study focused on 3-ply corrugated cardboards with grammages ranging from 350 to 550 g/m^2 and thicknesses from 1.5 mm to 4.0 mm.

All cardboard samples were conditioned in a climatic chamber under standardised laboratory conditions [43,44], specifically at a temperature of 23 °C and a relative humidity of 50%.

Material testing was conducted using a multifunctional device, the Box Strength Estimation (BSE) System [45], which, among others functions, served in determining the mechanical properties of cardboard. The following tests on cardboard samples were performed on the testing machine: the edge crush test, four-point bending test in two directions (the machine direction—BNT_{MD}; the cross-machine direction—BNT_{CD}), torsional stiffness test in two directions (TST_{MD} and TST_{CD}), and shear stiffness test.

For each type of cardboard, material testing was conducted on five sets of samples. One set of samples consisted of specimens for all tests conducted. All samples were cut using a Computer Numerical Control (CNC) laser device. Figure 2 presents images from the material testing procedures. The dimensions of the samples used in these tests are as follows:

- ECT: 100 × 25 mm;
- BNT_{MD} and BNT_{CD}: 250 × 50 mm;
- TST_{MD} and TST_{CD}: 150 × 30 mm;
- SST: 85 × 85 mm.

Figure 2. Material testing procedures: single set of cardboard samples and strength testing machine in the background.

Representative and averaged results from the material testing of all types of cardboard are presented in Table 1.

Table 1. Representative material data obtained through the mechanical testing of the corrugated boards selected for the study.

No.	*t* (mm)	*ECT* (kN/m)	*SST* (Nm)	TST_{CD} (Nm)	TST_{MD} (Nm)	BNT_{CD} (Nm)	BNT_{MD} (Nm)
1	1.52	5.08	0.59	0.24	0.25	0.41	0.91
2	1.52	5.70	0.75	0.31	0.31	0.51	1.27
3	1.68	5.82	0.86	0.37	0.38	0.65	1.60
4	2.86	4.88	1.02	0.73	0.55	1.69	2.80
5	2.99	6.20	1.36	0.96	0.79	2.16	4.13
6	2.96	7.00	1.54	1.09	0.86	2.33	5.05
7	3.90	5.23	1.70	1.21	0.73	3.25	4.58
8	3.88	5.47	1.88	1.25	0.81	3.37	6.51
9	3.99	6.12	2.27	1.58	0.91	4.66	7.4
10	2.80	3.71	0.84	0.61	0.42	1.33	2.29
11	2.93	6.22	1.15	0.84	0.67	1.93	3.47
12	3.01	7.27	1.52	1.09	0.89	2.47	4.84
13	3.91	5.08	1.86	1.40	0.75	3.50	5.88

Based on data obtained from the experimental campaign (Table 1), it was possible to calculate the material constants for the adopted constitutive model. An orthotropic material model was applied within the elastic range, along with directional plasticity through the use of Hill's potential. This model has demonstrated effectiveness in numerous previous scientific studies [30,39].

The material constants used in all numerical analyses of corrugated cardboard boxes considered in this work are presented in Table 2, where the following are shown:

- E_1, the elastic modulus in machine direction;
- E_2, the elastic modulus in cross-machine direction;
- ν_{12}, the Poisson's ratio;

- G_{12}, G_{13}, and G_{23}, the shear moduli;
- σ_0, the yield strength;
- R_{11}, the yield stress factor accounted for in the Hill's potential.

Table 2. Material constants used in the finite element analyses for modelling the mechanical properties of the corrugated boards selected for the study.

No.	E_1 (MPa)	E_2 (MPa)	ν_{12} (–)	G_{12} (MPa)	G_{13} (MPa)	G_{23} (MPa)	σ_0 (MPa)	R_{11} (–)
1	3383.8	1477.0	0.450	33241.2	2.283	2.125	3.346	0.951
2	4728.8	1788.6	0.483	43303.8	2.803	2.785	3.744	0.951
3	4423.5	1695.6	0.480	24813.0	3.141	3.074	3.459	0.951
4	1606.6	907.3	0.395	2719.86	2.845	4.007	1.708	0.774
5	2075.2	1016.7	0.424	2883.73	3.967	5.064	2.074	0.951
6	2663.2	1125.9	0.457	3617.59	4.298	5.725	2.369	0.951
7	1076.0	666.23	0.377	3068.41	2.572	4.677	1.332	0.501
8	1614.9	729.36	0.442	3575.25	2.883	4.884	1.407	0.634
9	1702.5	935.53	0.401	5589.19	3.076	5.761	1.533	0.867
10	1427.0	757.33	0.407	2753.01	2.1347	3.3672	1.323	0.550
11	1868.9	967.35	0.412	2593.59	3.4423	4.5821	2.127	0.800
12	2387.6	1137.7	0.430	3119.91	4.4628	5.749	2.416	0.800
13	1519.9	729.40	0.428	4352.27	2.6183	5.2937	1.312	0.800

2.3. Estimation of the Packaging Resistance to Transport Loads

According to the aims presented in the previous paragraphs, a numerical tool was developed for calculating changes in the compression strength of a specific box, following representative environmental vibrations experienced during transportation. As illustrated in [30], the process begins with a buckling analysis, to describe a possible numerical imperfection field, followed by a static FEA of the box in a stress-free state. This initial step allows for the determination of BCT_0^{ij}, which represents the compression strength of the box prior to the vertical random vibration test. Next, a modal analysis of the box is performed, and the results, along with Power Spectral Density (PSD) data, from standard ISO 13355 [24], serve as inputs for the random vibrations analysis.

In the subsequent step, a displacement boundary condition, corresponding to a specific resonant frequency, is applied to the bottom of the box during a dynamic analysis that simulates fixed-frequency vibrations. After a selected number of cycles, a quasi-static compression test is numerically conducted. This final analysis yields to the updated (reduced) BCT^{ij}, representing the compression strength of the box under a given transport condition, subjected to possible damages.

Both the static and dynamic analyses of box testing mirror laboratory test conditions. In the developed finite element models (see, Figure 3), only the quarter of load-bearing walls of the packaging are considered, while the bottom and top flaps are simulated by applying suitable boundary conditions, namely with out-of-plane displacements at the bottom and top edges of the sidewalls constrained.

The complete set of numerical analyses, conducted on the different models, account for three classes of simulations, namely random vibrations, static compressions and dynamic vibrations, which are also supported by buckling and modal analyses. Given the numerical difficulties related to the investigation of vertical random vibrations in the time domain, the research adopted an efficient approach for modelling the VRV test of corrugated board packaging, as proposed in [30], utilising modal analysis to identify resonant frequencies for subsequent employment in dynamic finite element analysis with a set vibration frequency.

The box compression test was simulated by applying a vertical displacement to the top edges of the box. In addition to the static model, a rigid plate was incorporated into the dynamic analysis to replicate the standardised load utilised in an experimental test. Moreover, the dynamic analysis consisted of two computational steps, i.e., the application of gravity, enforcing the plate to descend onto the packaging, with contact interaction, and the imposed vibration of the bottom of the box, in the time domain, with the sinusoidal amplitude and frequency derived from the modal analysis.

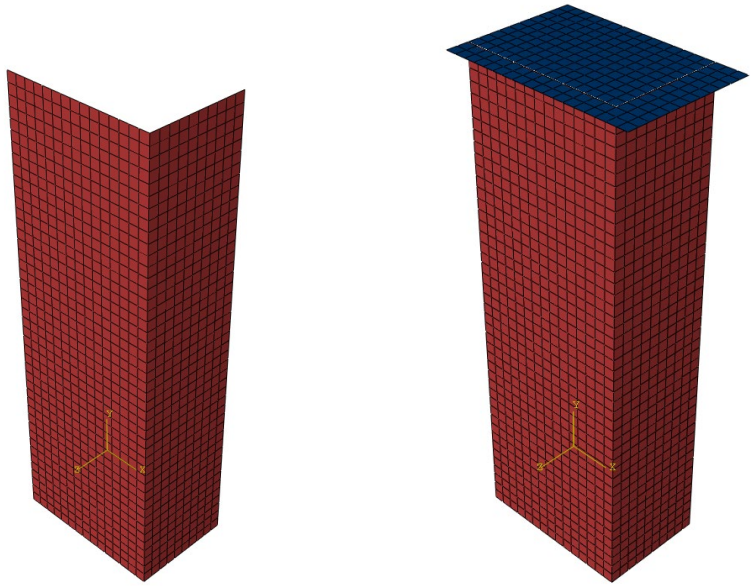

(**a**) (**b**)

Figure 3. Finite element models for (**a**) static and (**b**) dynamic analyses, here represented on a quarter geometry (box dimension III).

As introduced in previous sections, Sections 2.1 and 2.2, and in Figure 1, static and dynamic analyses were performed for thirteen corrugated board materials (Table 2) and three box geometries (Figure 1). In each run, the constitutive model employed was a linear elastic orthotropic material with Hill plasticity.

The numerical analyses and the gathered computational results collected in the following section, Section 3, were developed employing the finite element software Abaqus 2020 [46]. For the modelling of the corrugated board boxes, 4-node quadrilateral shell elements, with a full integration scheme, were utilised. The computational burden of the analyses was kept limited, without coarsening the accuracy of the results, by adopting a global mesh size of approximately 10 mm. Such an enriched set of analyses, accounting for various cardboard materials and diverse box geometries, allowed for global sensitivity analysis to facilitate the assessment and interpretation of the observed structural behaviour of packaging subjected to transport loads, as reported in the following Results and Discussion sections.

3. Results

According to the methodology presented above, the main numerical outcomes are gathered here, focusing on the reduction in box loadbearing capacity (ΔBCT^{ij}, %) after transportation, i.e., after possible damages due to impacts, assuming such mechanical measurements as reference indexes for the box structural response.

A complete set of numerical results are provided in Table 3, thoroughly summarising the thirty-nine analysed cases, for thirteen material selections (Tables 1 and 2) and three box designs (Figure 1). Thirteen types of materials were numbered from i = 1 to i = 13. Different box designs were labelled from j = I to j = III. The listed percentage reductions

allow for a direct reading and comparison of the response trends among the different cases. In particular, for increasing the reduction in the box compression test index, the box designs can be listed as II, I and III. Moreover, it can be observed that the lowest reductions are exhibited by materials No. 1 and 2, while the highest reductions are displayed by materials No. 9, 12 and 13. The data presented are discussed in details in Section 4.

Table 3. Percentage reduction (%) of box compression test index (ΔBCT^{ij}) for various materials (i = 1, 2, 3. . . 13) and dimensions (j = I, II, III); the highest reductions are highlighted in red and the lowest are highlighted in green.

Material	Dimension j = I	Dimension j = II	Dimension j = III
i = 1	2.14	0.72	2.52
i = 2	4.23	1.19	5.10
i = 3	5.50	1.98	6.43
i = 4	7.80	2.09	9.40
i = 5	9.98	2.48	11.8
i = 6	12.5	3.33	15.4
i = 7	9.64	2.08	10.7
i = 8	14.5	3.72	16.1
i = 9	17.0	5.65	19.2
i = 10	5.41	1.80	6.05
i = 11	7.09	2.38	7.66
i = 12	12.6	4.63	15.0
i = 13	15.1	3.93	18.1

The results are here revisited in graphical form (Figures 4–8). The main aim of the proposed plot is the investigation and interpretation of the box structural response, its trends and its possible correlations with material and structural parameters. The graphical outcomes reported in the current section are deemed the most significant, in terms of the intended aim, while the complete set of plotted data can be found in Appendix A.

Specifically, Figure 4 shows the variation in the reduction in strength, ΔBCT^{ij}, for diverse cardboard materials and box designs, offering an insight into the typical, representative trends and into the most significant responses. The radial axis denotes the reduction in the strength of the box, i.e., ΔBCT^{ij}, while the angular axis denotes the cardboards considered for particular boxes, from $i = 1$ to $i = 13$. The cardboards used are presented in Tables 1 and 2. Consistently with the differentiation for each box shape, Figures 5 and 6 focus on the possible relationship with cardboard structural parameters, including the following:

- thickness, (mm, t);
- ECT (kN/m);
- BNT_{CD} (Nm);
- BNT_{MD} (Nm).

The results gathered in Figure 5 display scattered outcomes with respect to cardboard thickness and the ECT index. Conversely, a possible correlation may be highlighted in the results presented in Figure 6, as specifically analysed and discussed in the following section, Section 4, which focuses on interpretations and comments on the results.

Figures 7 and 8 delve into possible correlations with cardboard mechanical constitutive parameters:

- E_1 (MPa);
- E_2 (MPa);
- σ_0 (MPa).

Although some global trends may be qualitatively observed, in Figures 7 and 8, between the constitutive mechanical parameters and the reduction in box load bearing capacity, the general scattering of the computed results prevents us from proposing any direct specific relationship. Such a structural response may be interpreted as a combined

effect of the material mechanical parameters and of the structural parameters including the panel and box scale size, with possibly competing detrimental and beneficial effects on the reduction in strength, ΔBCT^{ij}, this being a globally unified measure of the predicted structural response.

The data for the rest of the cardboard structural parameters and the rest of cardboard mechanical constitutive parameters are shown in Appendix A.

In order to develop a better understanding of the computed response, the observed data and results are discussed in the following section.

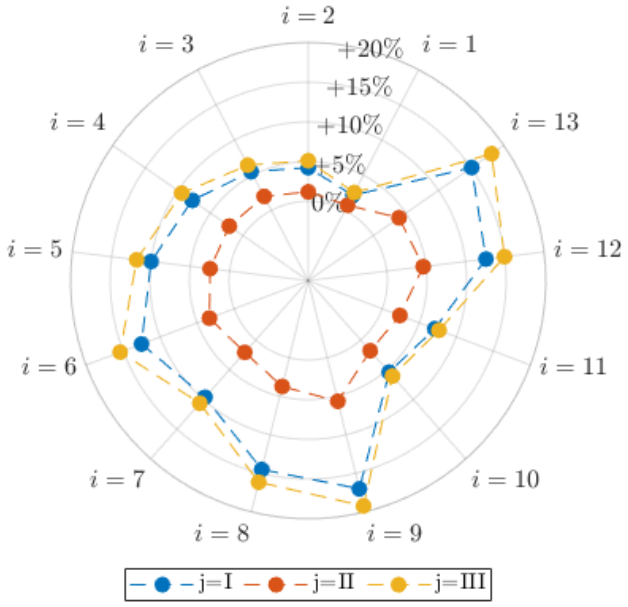

Figure 4. Percentage reduction (%) in box compression test index (ΔBCT^{ij}) for various materials (i = 1, 2, 3. . . 13) and dimensions (j = I, II, III).

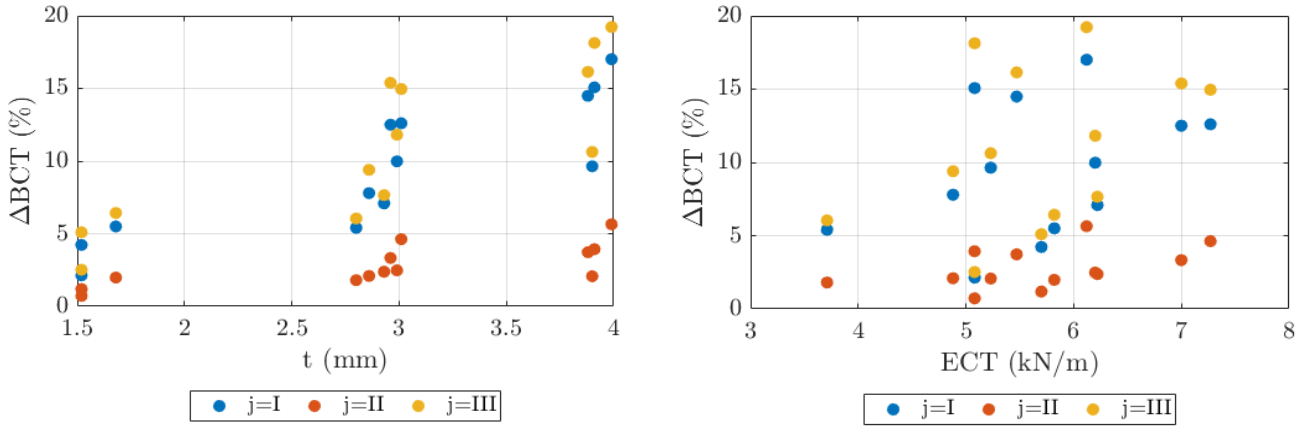

(**a**) (**b**)

Figure 5. Percentage reduction (%) in box compression test index (ΔBCT^{ij}) versus (**a**) cardboard thickness (mm, *t*) and versus (**b**) *ECT* (kN/m), for various materials (thirteen dots) and dimensions (j = I, II, III).

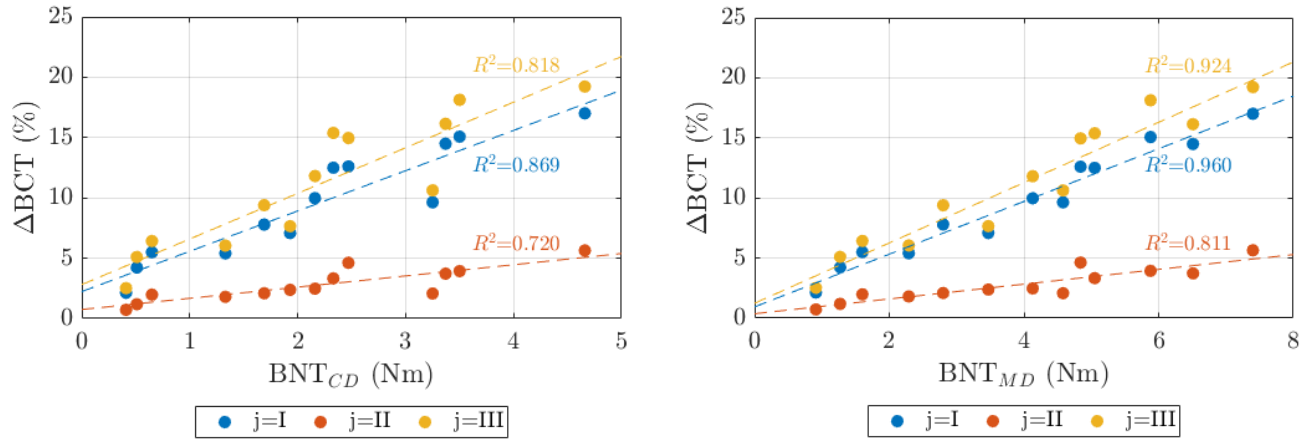

Figure 6. Percentage reduction (%) in box compression test index (ΔBCT^{ij}) versus (**a**) BNT_{CD} (Nm) and versus (**b**) BNT_{MD} (Nm), for various materials (thirteen dots) and dimensions (j = I, II, III).

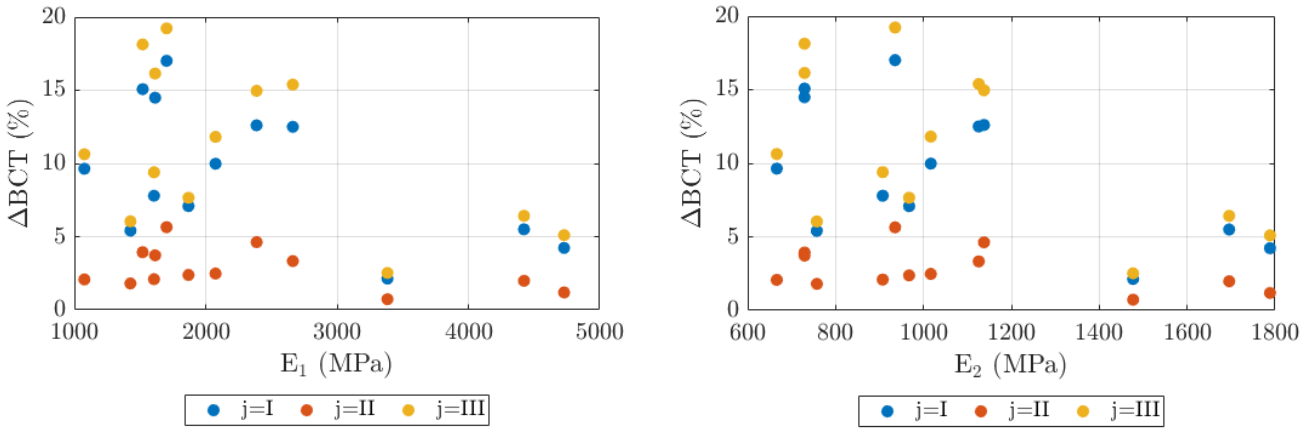

Figure 7. Percentage reduction (%) in box compression test index (ΔBCT^{ij}) versus (**a**) E_1 (MPa) and versus (**b**) E_2 (MPa), for various materials (thirteen dots) and dimensions (j = I, II, III).

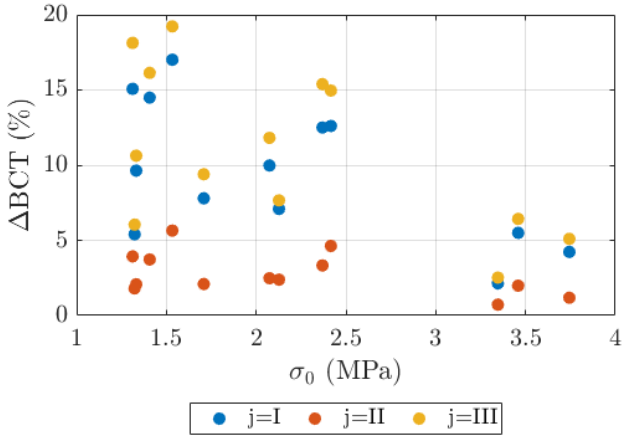

Figure 8. Percentage reduction (%) in box compression test index (ΔBCT^{ij}) versus σ_0 (MPa), for various materials (thirteen dots) and dimensions (j = I, II, III).

4. Discussion

The proposed methodology for the evaluation of the reduction in the box load-bearing capacity under transport loading conditions and possible consequent damages was extensively validated in [30]. Therefore, such an approach is effectively adopted in the present research, to deepen the understanding of and to further investigate the dependence of ΔBCT^{ij} on cardboard material structural and mechanical parameters, for various case combinations of cardboard materials and box geometries.

Since the transport loading condition may create permanent plastic deformations, buckling and damage in the packaging box, a consolidated understanding of the observed responses shall be developed through the interpretation of the structural behaviour of the analysed system, specifically for constitutive material properties, structural configurations, boundary conditions and loading effects. In particular, it is worth observing that material parameters may produce multiple effects related both to the anisotropic constitutive parameters of each layer and to the shell-homogenised mechanical parameters. Such features have been revealed to influence the expected box compression response from a material viewpoint. With respect to the numerically tested examples, this is observed when comparing the computational outcomes for varying cardboard materials (i = 1, 2, 3,. . .13). With regard to the mechanical constitutive parameters, the discussion of the gathered results may highlight that increases in mechanical properties (namely for higher quality constituent cardboard) tend to reduce the sensitivity of the box compression response to reduction effects.

Moreover, geometrical box design turns out to be a key parameter in influencing the extent of reduction in the box load-bearing capacity, where box sizes and shape ratios can significantly alter the structural response while varying the stiffness and strength of box cardboard side wall panels (i.e., structural shell elements). The numerical and graphical outcomes gathered in the previous section allow us to identify this behavioural response and its related trends under corresponding varying box designs (j = I, II, III). To reach more developed conclusions, it is worth observing that the constitutive material and structural effects may also be considered combined effects that mutually influence the box load bearing capacity and the possible reduction in it.

Among the investigated relationships and trends between constitutive constants (Table 2), material structural parameters (Table 1) and/or box designs (Figure 1) with the reduction in the box load bearing capacity, we will briefly discuss the seemingly linear correlation observed with the cardboard bending stiffness, focusing on the cardboard box sidewall bending stiffness of structural shells. Therefore, from the results obtained and summarised, it is possible to observe that the proposed globally unified measures of such structural responses and interpretations represent a guideline methodology for the assessment of the possible load bearing capacity reduction of cardboard boxes under transport load conditions, as well as an efficient approach for the structural interpretation of such conditions, for engineering research and industrial application.

One of the key conclusions of this study is that the reduction in compressive strength never exceeded 20%. This conclusion is a practical indication of what the impact of strength reductions due to transport loads in simple flap boxes with the aforementioned designs could be.

To the best of the authors' knowledge, no studies have addressed the reduction in box strength caused by transport loads. The available scientific literature includes studies that, at a more general level, evaluate the impact of various packaging transportation solutions, such as palletising methods, on sustainability [47]. However, more specific research directly addressing the aspects considered in this study remains unavailable. One of this study limitations is that the analysed boxes were reduced to the selected designs. Three shape ratios were chosen, which define the so-called American boxes, while other types of box designs were not considered. Additionally, the effects of holes or openings were excluded from the study. The numerical approach also only included double-symmetry and one-piece boxes.

5. Conclusions

This study examines the impact of different types of corrugated cardboard on the reduction in the compressive load-bearing capacity of packaging after exposure to standard transportation loads. Thirteen types of cardboard and three box designs were analysed using the finite element method to simulate both static and dynamic transport conditions, following the standards of applying vertical vibrations to simulate the conditions of packaging being transported. Mechanical tests on the cardboard materials, including edge crush and bending tests, provided data for modelling the material properties, with simulations accounting for plastic deformation and vibration effects. The results highlight how varied material properties influence the structural integrity of packaging differently, offering insights for optimising packaging resilience during transport.

One of the most interesting observations was that as the bending stiffness of the boards in the machine direction increased, the strength loss of the packaging due to transport loads also increased with an apparently linear trend. Other material constants, such as the ECT value, shear stiffness, torsional stiffness, and moduli of elasticity, did not show any significant or explicit correlation.

In view of possible future developments, the mechanical interpretation of the box compression response may provide an effective tool for the assessment of packaging transport and damage conditions, as well as for cardboard box design improvements, related to post-buckling design and detailing reinforcement through the use of accessories. Therefore, additional analyses are planned to examine more complex box designs, incorporating both strengthening elements, such as tapes, and weakening features, such as perforations and holes, to determine whether similar trends may be observed despite these modifications.

Author Contributions: Conceptualisation, T.G. (Tomasz Gajewski), T.G. (Tomasz Garbowski); methodology, D.M. and T.G. (Tomasz Gajewski); software, D.M. and. A.C.; validation, D.M. and A.K.-P.; formal analysis, A.C. and D.M.; investigation, A.C., D.M.; writing—original draft preparation, A.C., A.K.-P. and T.G. (Tomasz Gajewski); writing—review and editing, A.C., A.K.-P., T.G. (Tomasz Gajewski) and T.G. (Tomasz Garbowski); visualisation, A.C.; supervision, T.G. (Tomasz Garbowski) and T.G. (Tomasz Gajewski); project administration, T.G. (Tomasz Gajewski); funding acquisition, T.G. (Tomasz Garbowski). All authors have read and agreed to the published version of the manuscript.

Funding: The research was funded within the grant of The National Centre for Research and Development under the number POIR.01.01.01-00-0002/21.

Institutional Review Board Statement: Not applicable.

Informed Consent Statement: Not applicable.

Data Availability Statement: The data presented in this study are available on request from the corresponding author.

Acknowledgments: This work was published within the grant of The National Centre for Research and Development under the number POIR.01.01.01-00-0002/21.

Conflicts of Interest: The authors declare no conflicts of interest. The funders had no role in the design of the study; in the collection, analyses, or interpretation of data; in the writing of the manuscript, or in the decision to publish the results.

Appendix A

In addition to the graphical results presented in Section 3, this appendix reports on the completed set of data on the percentage reduction in the box compressive load bearing capacity (ΔBCT^{ij}) versus material data (refer to Table 1, in Figures A1 and A2) and versus material constitutive parameters (refer to Table 2, in Figures A3–A5).

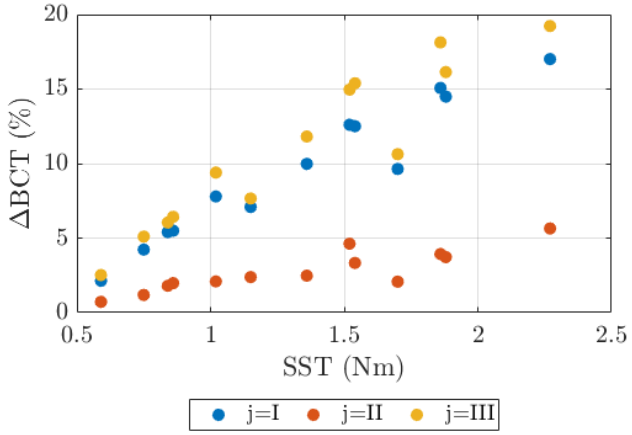

Figure A1. Percentage reduction (%) in the box compression test index (ΔBCT^{ij}) versus SST (Nm), for various materials (thirteen dots) and dimensions (j = I, II, III).

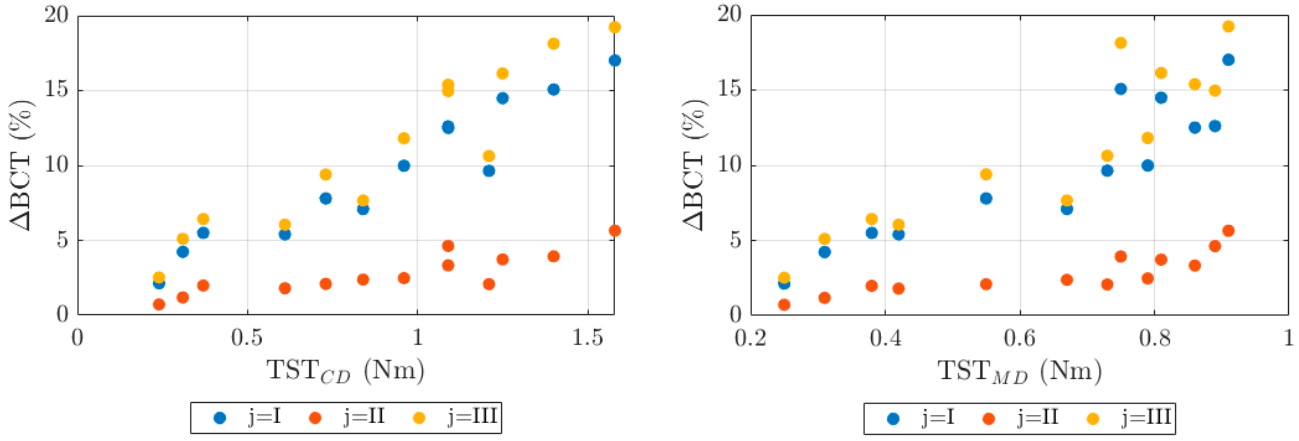

(**a**) (**b**)

Figure A2. Percentage reduction (%) in the box compression test index (ΔBCT^{ij}) versus (**a**) TST_{CD} (Nm) and versus (**b**) TST_{MD} (Nm), for various materials (thirteen dots) and dimensions (j = I, II, III).

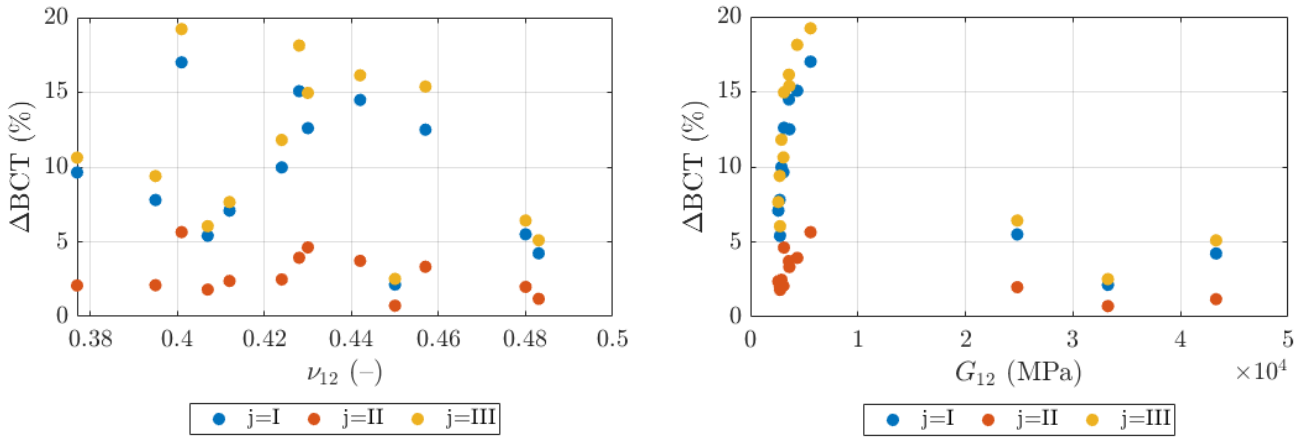

(**a**) (**b**)

Figure A3. Percentage reduction (%) in the box compression test index (ΔBCT^{ij}) versus (**a**) ν_{12} (−) and versus (**b**) G_{12} (MPa), for various materials (thirteen dots) and dimensions (j = I, II, III).

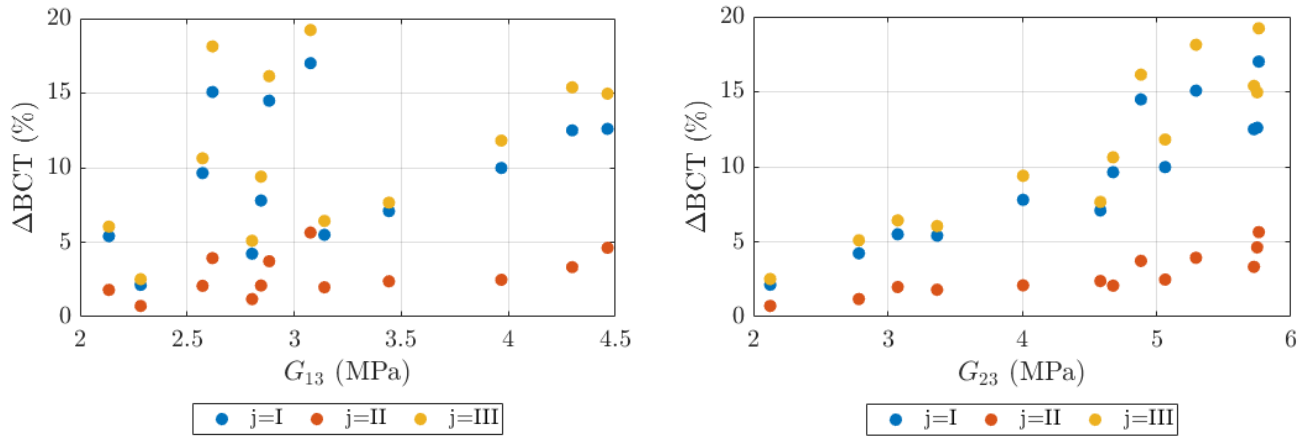

(**a**) (**b**)

Figure A4. Percentage reduction (%) in the box compression test index (ΔBCT^{ij}) versus (**a**) G_{13} (MPa) and versus (**b**) G_{23} (MPa), for various materials (thirteen dots) and dimensions (j = I, II, III).

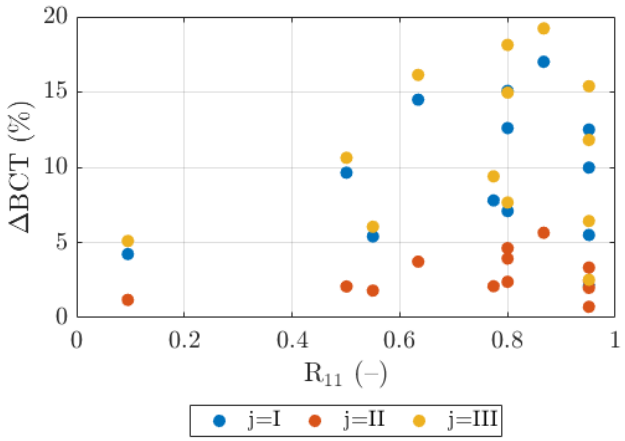

Figure A5. Percentage reduction (%) in the box compression test index (ΔBCT^{ij}) versus R_{11} (−), for various materials (thirteen dots) and dimensions (j = I, II, III).

References

1. Bajpai, P. Basic Overview of Pulp and Paper Manufacturing Process. In *Green Chemistry and Sustainability in Pulp and Paper Industry*, 1st ed.; Bajpai, P., Ed.; Springer: Cham, Switzerland, 2015. [CrossRef]
2. Pereira, T.; Neves, A.S.L.; Silva, F.J.G.; Godina, R.; Morgado, L.; Pinto, G.F.L. Production Process Analysis and Improvement of Corrugated Cardboard Industry. *Procedia Manuf.* **2020**, *51*, 1395–1402. [CrossRef]
3. Kaushal, M.; Sirohiya, V.; Rathore, R. Corrugated board structure: A review. *Int. J. Appl. Eng. Technol.* **2015**, *2*, 228–234.
4. Kellicutt, K.; Landt, E. Development of design data for corrugated fibreboard shipping containers. *Tappi* **1952**, *35*, 398–402.
5. Maltenfort, G. Compression strength of corrugated containers. *Fibre Contain.* **1956**, *41*, 106–121.
6. McKee, R.C.; Gander, J.W.; Wachuta, J.R. Compression strength formula for corrugated boxes. *Paperboard Packag.* **1963**, *48*, 149–159.
7. Urbanik, T.J.; Frank, B. Box compression analysis of world-wide data spanning 46 years. *Wood Fiber Sci.* **2006**, *38*, 399–416.
8. Allerby, I.M.; Laing, G.N.; Cardwell, R.D. Compressive strength—From components to corrugated containers. *Appita Conf. Notes* **1985**, *1*, 1–11.
9. Batelka, J.J.; Smith, C.N. *Package Compression Model*; Institute of Paper Science and Technology: Atlanta, GA, USA, 1993.
10. Ristinmaa, M.; Ottosen, N.S.; Korin, C. Analytical Prediction of Package Collapse Loads-Basic considerations. *Nord. Pulp Pap. Res. J.* **2012**, *27*, 806–813. [CrossRef]
11. Schrampfer, K.E.; Whitsitt, W.J.; Baum, G.A. *Combined Board Edge Crush (ECT) Technology*; Institute of Paper Chemistry: Appleton, WI, USA, 1987.
12. Garbowski, T.; Knitter-Piątkowska, A. Analytical Determination of the Bending Stiffness of a Five-Layer Corrugated Cardboard with Imperfections. *Materials* **2022**, *15*, 663. [CrossRef]

13. Fadiji, T.; Coetzee, C.J.; Opara, U.L. Compression strength of ventilated corrugated paperboard packages: Numerical modelling, experimental validation and effects of vent geometric design. *Biosyst. Eng.* **2016**, *151*, 231–247. [CrossRef]
14. Słonina, M.; Dziurka, D.; Smardzewski, J. Experimental research and numerical analysis of the elastic properties of paper cell cores before and after impregnation. *Materials* **2020**, *13*, 2058. [CrossRef] [PubMed]
15. Fadiji, T.; Ambaw, A.; Coetzee, C.J.; Berry, T.M.; Opara, U.L. Application of finite element analysis to predict the mechanical strength of ventilated corrugated paperboard packaging for handling fresh produce. *Biosyst. Eng.* **2018**, *174*, 260–281. [CrossRef]
16. Suarez, B.; Muneta, M.L.M.; Sanz-Bobi, J.D.; Romero, G. Application of homogenization approaches to the numerical analysis of seating made of multi-wall corrugated cardboard. *Compos. Struct.* **2021**, *262*, 113642. [CrossRef]
17. Frank, B. Corrugated box compression—A literature survey. *Packag. Technol. Sci.* **2014**, *27*, 105–128. [CrossRef]
18. Jamsari, M.A.; Kueh, C.; Gray-Stuart, E.M.; Dahm, K.; Bronlund, J.E. Modelling the impact of crushing on the strength performance of corrugated fibreboard. *Packag. Technol. Sci.* **2020**, *33*, 159–170. [CrossRef]
19. Bai, J.; Wang, J.; Pan, L.; Lu, L.; Lu, G. Quasi-static axial crushing of single wall corrugated paperboard. *Compos. Struct.* **2019**, *226*, 111237. [CrossRef]
20. Garbowski, T.; Knitter-Piątkowska, A.; Grabski, J.K. Estimation of the Edge Crush Resistance of Corrugated Board Using Artificial Intelligence. *Materials* **2023**, *16*, 1631. [CrossRef]
21. Rogalka, M.; Grabski, J.K.; Garbowski, T. Identification of Geometric Features of the Corrugated Board Using Images and Genetic Algorithm. *Sensors* **2023**, *23*, 6242. [CrossRef]
22. Garbowski, T.; Grabski, J.K.; Marek, A. Full-field measurements in the edge crush test of a corrugated board—Analytical and numerical predictive models. *Materials* **2021**, *14*, 2840. [CrossRef]
23. Viguié, J.; Dumont, P.J.J. Analytical post-buckling model of corrugated board panels using digital image correlation measurements. *Comp. Struct.* **2013**, *101*, 243–254. [CrossRef]
24. *ISO 13355:2016*; Packaging—Complete, Filled Transport Packages and Unit Loads—Vertical Random Vibration Test. International Organization for Standardization: Geneva, Switzerland, 2016.
25. Abbès, B.; Guo, Y.Q. Analytic homogenization for torsion of orthotropic sandwich plates. *Appl. Comp. Struct.* **2010**, *92*, 699–706. [CrossRef]
26. Gallo, J.; Cortés, F.; Alberdi, E.; Goti, A. Mechanical behavior modeling of containers and octabins made of corrugated cardboard subjected to vertical stacking loads. *Materials* **2021**, *14*, 2392. [CrossRef] [PubMed]
27. Mrówczyński, D.; Knitter-Piątkowska, A.; Garbowski, T. Numerical Homogenization of Single-Walled Corrugated Board with Imperfections. *Appl. Sci.* **2022**, *12*, 9632. [CrossRef]
28. Guo, Y.; Xu, W.; Fu, Y.; Zhang, W. Comparison studies on dynamic packaging properties of corrugated paperboard pads. *Engineering* **2010**, *2*, 378–386. [CrossRef]
29. Osowski, P.; Piątkowski, T. Analysis of corrugated cardboard influence on the protective properties of complex packaging system. *AIP Conf. Proc.* **2017**, *1822*, 020011. [CrossRef]
30. Mrówczyński, D.; Gajewski, T.; Garbowski, T. A Simplified Dynamic Strength Analysis of Cardboard Packaging Subjected to Transport Loads. *Materials* **2023**, *16*, 5131. [CrossRef]
31. Zambujal-Oliveira, J.; Fernandes, C. The Contribution of Sustainable Packaging to the Circular Food Supply Chain. *Packag. Technol. Sci.* **2024**, *37*, 443–456. [CrossRef]
32. Jannes, R.; Vanhauwaemeiren, P.; Slaets, P.; Juwet, M. Assessing the Sustainable Potential of Corrugated Board-Based Bundle Packaging of PET Bottles: A Life Cycle Perspective—A Case Study. *Clean. Technol.* **2023**, *5*, 1214–1234. [CrossRef]
33. Chen, J.; Zhang, Y.; Sun, J. An overview of the reducing principle of design of corrugated box used in goods packaging. *Procedia Environ. Sci.* **2011**, *10*, 992–998. [CrossRef]
34. Wang, C.-C.; Chen, C.-H.; Jiang, B.C. Shock absorption characteristics and optimal design of corrugated fiberboard using drop testing. *Appl. Sci.* **2021**, *11*, 5815. [CrossRef]
35. Mrówczyński, D.; Garbowski, T.; Knitter-Piątkowska, A. Estimation of the compressive strength of corrugated board boxes with shifted creases on the flaps. *Materials* **2021**, *14*, 5181. [CrossRef] [PubMed]
36. Wang, L.-J.; Lai, Y.-Z.; Wang, Z.-W. Fatigue failure and Grms–N curve of corrugated paperboard box. *J. Vib. Control* **2020**, *26*, 1028–1041. [CrossRef]
37. Garbowski, T. Evaluating safety factors in corrugated packaging for extreme environmental conditions. *Packag. Rev.* **2023**, *4*, 6–15.
38. Khan, D.; Burdzik, R. Measurement and analysis of transport noise and vibration: A review of techniques, case studies, and future directions. *Measurement* **2023**, *220*, 113354. [CrossRef]
39. Mrówczyński, D.; Gajewski, T.; Pośpiech, M.; Garbowski, T. Estimation of the Compressive Strength of Cardboard Boxes Including Packaging Overhanging on the Pallet. *Appl. Sci.* **2024**, *14*, 819. [CrossRef]
40. Sonnenberg, S.A.J.; Rocha, J.; Misol, M.; Rose, M. Experimental validation of an acceleration power spectral density aircraft panel model given different excitations. *Can. Acoust.-Acoust. Can.* **2018**, *46*, 19–30.
41. Ketkale, H.; Simske, S.J. A LifeCycle Analysis and Economic Cost Analysis of Corrugated Cardboard Box Reuse and Recycling in the United States. *Resources* **2023**, *12*, 22. [CrossRef]
42. Chowdhury, T.; Kabir, G. Lifecycle Assessment (LCA) of Package Deliveries: Sustainable Decision-Making for the Academic Institutions. *Green Low-Carbon Econ.* **2024**, *2*, 1–13. [CrossRef]

43. *ISO 187:2022*; Paper, Board and Pulps—Standard Atmosphere for Conditioning and Testing and Procedure for Monitoring the Atmosphere and Conditioning of Samples. International Organization for Standardization: Geneva, Switzerland, 2022.
44. *TAPPI T402 sp-21*; Standard Conditioning and Testing Atmospheres for Paper, Board, Pulp Handsheets, and Related Products, Test Method TAPPI/ANSI T 402 sp-21. TAPPI Press: Atlanta, GA, USA, 2021.
45. FEMAT. FEMat Systems: BSE System. Available online: http://fematsystems.pl/bse-system_en (accessed on 24 October 2024).
46. Dassault Systèmes. Abaqus Unified FEA® Software. Available online: https://www.3ds.com/products-services/simulia/products/abaqus (accessed on 24 October 2024).
47. Kim, S.; Horvath, L.; Russell, J.D.; Park, J. Sustainable and Secure Transport: Achieving Environmental Impact Reductions by Optimizing Pallet-Package Strength Interactions during Transport. *Sustainability* **2023**, *15*, 12687. [CrossRef]